Mediators of Glioblastoma Resistance and Invasion during Antivascular Endothelial Growth Factor Therapy

Agda K. Lucio-Eterovic, Yuji Piao, and John F. de Groot

Abstract

Purpose: Vascular endothelial growth factor (VEGF) has been identified as a critical regulator of angiogenesis. Currently, several different strategies are being used to target the VEGF-VEGF receptor signal transduction pathway in glioblastoma. Although anti-VEGF therapy seems be effective in normalizing abnormal tumor vasculature, leading to an enhanced response to radiation and chemotherapy, tumors eventually become resistant to the therapy and adopt a highly infiltrative and invasive phenotype.

Experimental Design: In the present study, we evaluated the effects of anti-VEGF therapy (bevacizumab) on glioblastoma invasion both *in vitro* and *in vivo* and evaluated the angiogenesis- and invasion-related mediators of developed resistance to this therapy.

Results: We found that glioblastoma tumors escaped from antiangiogenic treatment by (*a*) reactivating angiogenesis through up-regulation of other proangiogenic factors and (*b*) invading normal brain areas, which was seen in association with up-regulation of matrix metalloproteinase (MMP)-2, MMP-9, and MMP-12; secreted protein, acidic, cysteine-rich; and tissue inhibitor of metalloproteinase 1. In addition to the paracrine effects of VEGF on endothelial cells, autocrine VEGF signaling seemed to regulate glioblastoma invasion because anti-VEGF therapy increased tumor invasiveness *in vitro*.

Conclusions: Collectively, these findings reinforce the importance of VEGF in regulating tumor invasion and identify potential mediators of resistance to targeted VEGF therapy. These results will be important for developing novel combination therapies to overcome this resistance phenotype.

Angiogenesis is one pathologic hallmark of glioblastoma tumors, the most aggressive and lethal form of brain cancer. This process consists of the formation of new blood vessels from preexisting ones, and it is a crucial step in the progression of cancer from a small and localized neoplasm to a highly aggressive tumor. Angiogenesis is regulated by the balance between many proangiogenic and antiangiogenic factors. Among them, vascular endothelial growth factor (VEGF) has been identified as the most critical molecule involved. VEGF ligands (VEGF-A, VEGF-B, VEGF-C, VEGF-D, and placenta growth factor) bind to and activate the VEGF receptor (VEGFR) tyrosine kinases [VEGFR-1 (also called Flt-1) and VEGFR-2 (also called Flk-1 or KDR)] expressed by endothelial cells in a paracrine manner. VEGF also interacts with the coreceptors neurophilin-1 and neurophilin-2. Binding of VEGF to VEGFR-2 receptors on endothelial cells initiates a signaling cascade that leads to proliferation, survival, and migration of endothelial cells (1, 2). In addition, the existence of autocrine VEGF signaling in cancer has been previously shown (3–5). VEGF stimulation of VEGFRs on glioma cells has been shown to be important for cell survival and proliferation (4).

Several studies have shown that the interaction between VEGF and its receptors can be antagonized by monoclonal antibodies to VEGF and small-molecule inhibitors of the VEGFR (6–8). It has been hypothesized that these agents are effective because the anti-VEGF treatment transiently normalizes abnormal tumor blood vessels (which leads to improved tumor oxygenation, enhancing response to radiotherapy ref. 9) and improves the delivery of chemotherapeutic drugs (10, 11). The most developed and successful treatment to date for recurrent glioblastoma is the VEGF-neutralizing antibody bevacizumab. In combination with chemotherapy, bevacizumab improves the progression-free survival or prolongs the survival of patients with lung, colon, or breast cancer (12). This combination of bevacizumab and irinotecan has recently been shown to improve the progression-free survival rate of patients with recurrent malignant gliomas (13) and also increase median survival (14).

Antiangiogenic therapy is effective in blocking vascular permeability, inhibiting vascular proliferation, and slowing tumor growth, but studies in multiple cancer types, including breast cancer (15), colorectal cancer (16), and pancreatic cancer (17), have shown that resistance to anti-VEGF therapy is the rule. The mechanisms by which this resistance occurs are not well understood but are thought to relate to alternative pathway activation. Several studies have shown that glioma xenografts

Authors' Affiliation: Brain Tumor Center, Department of Neuro-Oncology, The University of Texas M. D. Anderson Cancer Center, Houston, Texas

Received 3/6/09; revised 4/13/09; accepted 4/15/09; published OnlineFirst 6/30/09.

Grant support: An American Society of Clinical Oncology Career Development Award (J. de Groot) and the Martha G. Williams Brain Tumor Research Fund.

The costs of publication of this article were defrayed in part by the payment of page charges. This article must therefore be hereby marked *advertisement* in accordance with 18 U S.C. Section 1734 solely to indicate this fact.

Requests for reprints: John de Groot, Department of Neuro-Oncology, The University of Texas M. D. Anderson Cancer Center, 1515 Holcombe Boulevard, Unit 431, Houston, TX 77030. Phone: 713-792-7255; Fax: 713-794-4999; E-mail: jdegroot@mdanderson.org.

doi:10.1158/1078-0432.CCR-09-0575

Translational Relevance

Antiangiogenic therapy is commonly being used for the treatment of recurrent glioblastoma. Although there is strong evidence supporting the efficacy of this approach, tumors eventually acquire resistance to continuous blockade of blood vessel growth. We show that anti – vascular endothelial growth factor (VEGF) therapy promotes the expression of multiple proangiogenic and proinvasive factors that mediate glioma tumor escape. In particular, we show that anti-VEGF therapy significantly increases the expression of metalloproteinases, which are known to be important for the degradation of tumor stroma, for the release of VEGF and other proangiogenic factors bound to the extracellular matrix, and for facilitating tumor invasion. Inhibition of matrix metalloproteinases together with anti-VEGF therapy prolonged animal survival in an orthotopic glioma model but did not inhibit tumor invasion. These studies provide important information about the effect of anti-VEGF therapy on tumor evasion and resistance and help inform future clinical trials using novel drug combinations.

adopt a more invasive pattern of tumor growth via host vessel co-option when treated with anti-VEGF or anti-VEGFR antibodies (18, 19). Recently, the same pattern of tumor infiltration has been described in patients (20), although no pathologic evidence of vessel co-option has been reported. The mediators of this tumor invasion are currently unknown.

In the present study, we used a monoclonal antibody against VEGF (bevacizumab) to investigate the effects of antiangiogenic treatment on glioblastoma proliferation and invasion *in vitro* and *in vivo*. Secreted proteins and cellular changes were measured before and after anti-VEGF therapy in two cell lines and an orthotopic mouse model to determine mediators of resistance and invasion promoted by this treatment.

Materials and Methods

Cell lines, reagents, and treatment. Human glioblastoma cell line U87 was obtained from American Type Culture Collection. Glioma stem cell line NSC23 was obtained from Dr. Howard Colman (Department of Neuro-Oncology, M.D. Anderson Cancer Center, Houston, TX). U87 cells were maintained in DMEM containing 10% fetal bovine serum, and NSC23 cells were maintained in suspension in DMEM containing epidermal growth factor, basic fibroblast growth factor (bFGF), and B27 (Invitrogen) at 37°C in 5% CO_2 atmosphere. For cell treatment, human IgG was used as a control for all experiments, and bevacizumab was added at the concentrations indicated (see figures).

The primary antibodies used in this study were matrix metalloproteinase (MMP) 2; hypoxia inducible factor (HIF)-2α (Chemicon-Millipore); tissue inhibitor of MMP (TIMP)-1 (R&D Systems); MMP-9 (R&D Systems); MMP-12 (Abcam); secreted protein, acidic, cysteine-rich (SPARC; Zymed-Invitrogen); carbonic anhydrase IX (CA IX; Novus Biological); factor VIII (DAKO); Ki-67 (Santa Cruz Biotechnology); and bFGF (Calbiochem). VEGF levels were evaluated using the colorimetric sandwich ELISA method (R&D Systems). Free VEGF was measured using an immunodepletion method as previously described (21).

Invasion assay. Matrigel Basement Membrane Matrix (BD Labware) was used to perform the *in vitro* cell invasion assays. Cells were pretreated with bevacizumab for 72 h. Transwell inserts for 24-well plates were coated with diluted Matrigel, and cells were added in triplicate to the transwells. Serum-free medium was added to the bottom of the plate. Bevacizumab, at indicated concentrations, was added to both the upper and bottom chambers of the Matrigel system. Cells were allowed to invade for 24 h at 37°C. The filters were then fixed and stained with 0.1% crystal violet in 20% methanol. The invasive cells were visualized using bright-field microscopy. Transwell membranes were incubated with 2% deoxycholic acid for 20 min, and the absorbance at 595 nm was recorded.

Antibody and real-time PCR arrays. For the analysis of secreted proteins, we used the angiogenesis antibody array (Panomics) following the manufacturer's protocol. Two-milliliter aliquots of conditioned media were used for control and treated membranes. To verify changes in gene expression of control and treated cells, angiogenesis and extracellular matrix (ECM) real-time PCR arrays (SABiosciences) were carried out according to the manufacturer's protocol. Total cellular RNA was extracted using Trizol reagent (Invitrogen), and RNA was reverse transcribed to single-stranded cDNA using the High Capacity cDNA Reverse Transcription Kit (Applied Biosystems) according to the manufacturer's protocol. The experiment was carried out using Chromo4 (Bio-Rad) real-time PCR equipment. The extent of change in expression of each gene was calculated using the ΔC_t method.

Gelatin zymography. SDS-PAGE was done using 8% total acrylamide under reducing or nonreducing conditions, as previously described (22). For zymography analysis, aliquots of the conditioned media in 4× SDS loading buffer were loaded without reduction in 0.1% gelatin in 8% acrylamide gels. After electrophoresis, gels were washed with 2.5% Triton X-100 to remove SDS and renature the MMPs. Then the gels were incubated in developing buffer [2.5% Triton X-100 in 50 mmol/L Tris (pH 7.5), 150 mmol/L NaCl, and 10 mmol/L $CaCl_2$] overnight at 37°C to induce gelatin lysis by renatured MMPs. Gels were stained in a Coomassie brilliant blue solution and then destained with 30% methanol and 10% acetic acid.

Western blotting. For protein analysis by Western blotting, 30 μg of protein for each sample were loaded and separated by SDS-PAGE (22). Proteins were transferred onto nitrocellulose membranes, and the membranes were blocked in 5% bovine serum albumin. The primary antibodies were diluted in TBS with Tween 20 (TBST) containing 5% bovine serum albumin, and the membranes were incubated for 1 h at room temperature. The membranes were then washed thrice with TBST, incubated with the respective secondary antibody, and washed thrice with TBST. The secondary antibody was visualized using electron chemiluminescent reagent (Pierce).

Immunofluorescence. Immunofluorescence analysis was done as previously described with minor modifications (23). Briefly, formaldehyde-fixed cells were permeabilized with Triton X-100 0.3% in PBS, treated with Image-iT FX signal enhancer (Invitrogen) for 30 min, and blocked with 5% serum diluted in PBS-gel (0.2% gelatin in PBS) for 30 min. The primary antibodies were incubated in blocking solution for 1 h at room temperature. Alexa Fluor 488 – labeled goat anti-mouse MMP-2 and Alexa Fluor 594 – labeled donkey anti-goat MMP-9 antibodies (Molecular Probes, Invitrogen) were used to detect fluorescence. The coverslips were mounted using ProLong antifade reagent (Invitrogen). The images were acquired with an inverted deconvolution microscope. Images were taken with a Zeiss Axioskop 40 microscope equipped with AxioVision Rel.4.2 software.

Animal xenografts. For *in vivo* experiments, U87 glioblastoma cells (5×10^5) were implanted intracranially into nude mice (six mice per group). Beginning 4 d after implantation, animals were treated with bevacizumab (10-20 mg/kg i.p.) twice weekly. One group was treated for 4 wk (short-term treatment), and another group was treated until they required euthanasia, at ~7 wk (long-term treatment). In a separate experiment, after injection of U87 glioblastoma cells, animals were treated with bevacizumab alone or bevacizumab in combination with MMP inhibitors doxycycline (10 mg in the form of a slow-release s.c. pellet implant; Innovative Research of America) or GM 6001

(100 mg/kg i.p. thrice a week; Chemicon). Control animals were treated with PBS. When the mice developed signs and symptoms of advanced tumors, they were euthanized, and their brains were removed and processed for analysis. All experiments were approved by the Institutional Animal Care and Use Committee of The University of Texas M. D. Anderson Cancer Center. Survival analysis was done using the Kaplan-Meier method and groups were compared using the log-rank test. $P < 0.05$ was determined to be significant.

Immunohistochemistry. Paraffin sections from xenografts were used for immunohistochemical analysis. The slides were deparaffinized and subjected to graded rehydration. After blocking in 5% serum and an antigen retrieval step (citrate buffer, pH 6.0), the slides were incubated with the primary antibodies for 1 h at room temperature. After washing in PBS with Tween 20, primary antibody reactions were detected using the Vectastain ABC kit (Vector Laboratories) with the respective secondary antibody.

Results

***Immunodepletion of VEGF increased invasion of glioblastoma cells* in vitro.** Because antiangiogenic therapy has been shown to increase glioblastoma invasion *in vivo* (18, 19), we first isolated the impact of blocking the autocrine VEGF effect on tumor cell invasion. Two glioma cell lines (U87 glioblastoma cells and NSC23 glioma stem cells), which both release high levels of VEGF and have minimal or no *in vitro* or *in vivo* invasion, were selected for treatment with bevacizumab. To confirm the sequestration of soluble free VEGF after bevacizumab treatment, free VEGF levels were measured in the conditioned media following immunodepletion of VEGF bound to bevacizumab. A concentration of 5 mg/mL bevacizumab sequestered 98% of free VEGF in U87 cells and 90% of free VEGF in NSC23 cells at 72 hours (Fig. 1A).

To determine the baseline expression of VEGFRs available for autocrine stimulation on glioma cells, we measured the mRNA and protein levels of VEGFRs VEGFR-1 and VEGFR-2 by real-time PCR and Western blotting, respectively, in U87 and NSC23 cells. Figure 1B and Table 1 shows the protein and mRNA levels for these receptors. At the protein level, we detected high levels of VEGFR-1 and very low levels of VEGFR-2 in both cell lines. Interestingly, a clear down-regulation of VEGFR-1 was found in NSC23 cells after bevacizumab treatment. mRNA levels for VEGFR-1 and VEGFR-2 were not significantly different before and after anti-VEGF treatment.

We then investigated the effect of anti-VEGF treatment on the ability of glioblastoma cells to invade. A Matrigel transwell assay showed increased transwell migration/invasion for both treated U87 cells and treated NSC23 cells in a concentration-dependent manner. Compared with the numbers of invasive

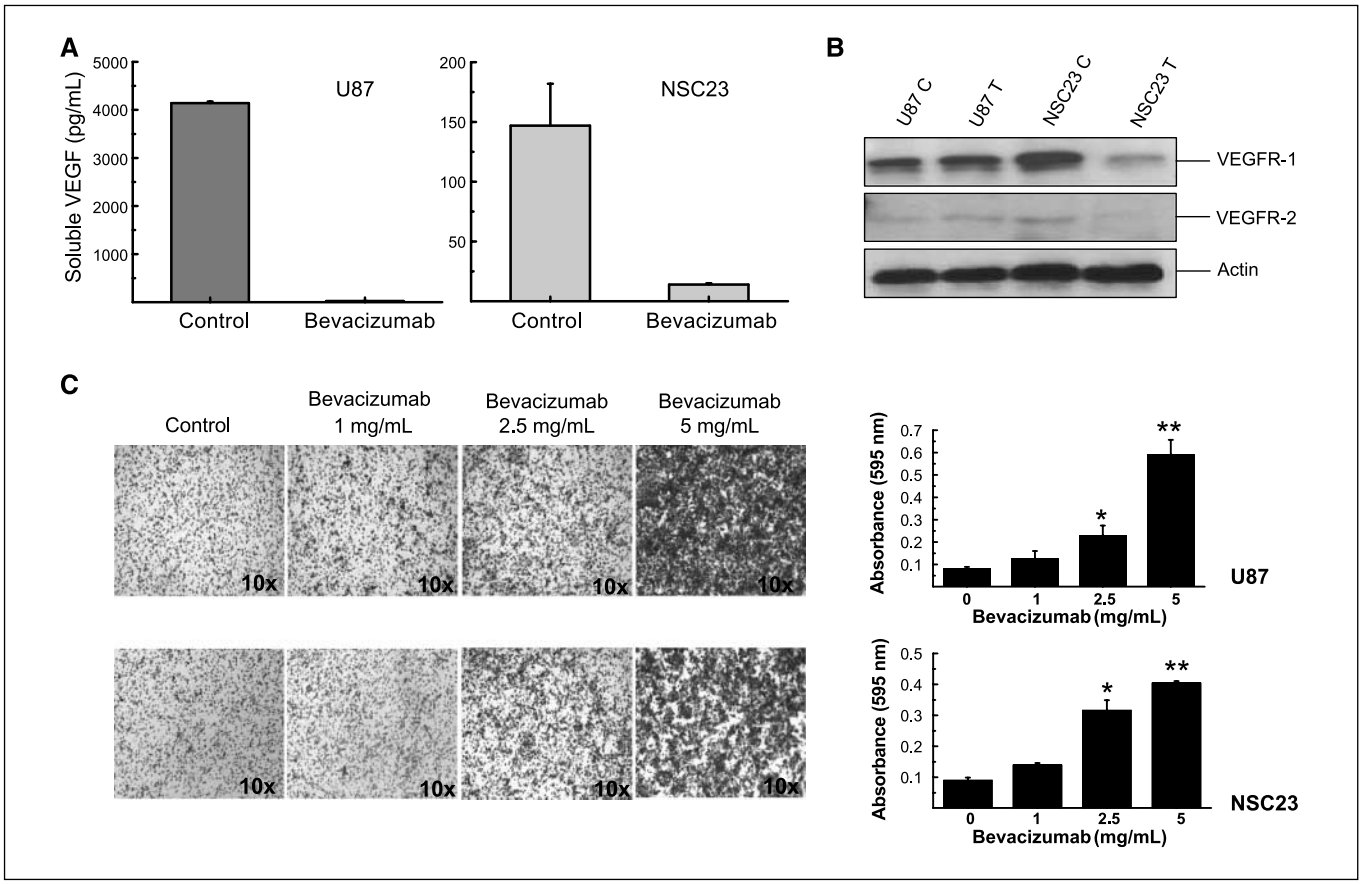

Fig. 1. Invasion increases *in vitro* following VEGF sequestration with bevacizumab. *A,* secreted VEGF levels measured by ELISA using conditioned media from control and bevacizumab-treated (5 mg/mL for 72 h) U87 and NSC23 cells after immunodepletion. Columns, average from three independent measurements. *B,* mRNA (ΔC_t) and protein levels of VEGFR-1 and VEGFR-2 in U87 and NSC23 cells. *C*, control cells; T, treated (5 mg/mL for 72 h) cells. *C,* Matrigel invasion assay for U87 (*top row*) and NSC23 (*bottom row*) cells. After 72 h of treatment with the indicated drug concentrations, cells (2.5×10^5) were allowed to invade for 24 h in serum-free medium. Graphs represent absorbance at 595 nm after incubation of the membranes with deoxycholic acid. Pictures shown are the most representative from three independent experiments. *, $P < 0.05$; **, $P < 0.01$, compared with control (Student's *t* test).

Table 1. VEGFR-1 and VEGFR-2 levels in U87 and NSC23 cells

	U87		NSC23	
	C	T	C	T
VEGFR-1	9.09	12.7	3.54	4.82
VEGFR-2	8.12	9.49	5.61	3.46

Abbreviations: C, control cells; T, treated cells.

control cells, the numbers of invasive cells were six times (U87) and four times (NSC23) higher when the cells were treated with 5 mg/mL bevacizumab (Fig. 1C), suggesting that autocrine VEGF signaling blockade plays an important role in glioma invasion. To ensure that changes in invasiveness were not a result of an imbalance in cell viability induced by bevacizumab treatment, cell viability was measured before each invasion experiment. Control and treated cells exhibited similar levels of viability after 72 hours, indicating that the treatment had not promoted the selection of resistant and invasive populations (data not shown).

Angiogenesis treatment alters the expression of multiple angiogenesis- and invasion-related genes. To identify potential mediators involved in the more invasive pattern shown *in vitro* (and *in vivo*, as described below) after antiangiogenic treatment, we used a quantitative real-time reverse transcription PCR array to screen for changes in mRNA levels of angiogenesis- and invasion-related genes. Table 2 shows the genes that are up-regulated and down-regulated after bevacizumab treatment. *MMP-12*, collagen type IV, α3 (*COL4-A3*), and chemokine-9 (*CXCL9*) were the most up-regulated genes (changes from 38- to 78-fold). *MMP-9*, another important angiogenesis- and invasion-related gene, was found to be expressed at a level ~11 times higher in the treated cells than in the control cells. On the other hand, laminin α1 (*LAMA1*), integrin β_2 (*ITGB2*), *MMP-1*, and hyaluronan synthase 1 (*HAS1*) were found to be down-regulated after bevacizumab treatment (changes from 19- to 54-fold).

To validate the higher mRNA levels shown by real-time PCR, we used immunofluorescence and Western blotting to analyze

Table 2. mRNA changes after anti-VEGF treatment in U87 glioblastoma cell line

Unigene	Symbol	Description	Fold change (treated/control)
Genes up-regulated			
Hs.369675	*ANGPT1*	Angiopoietin 1	7.96
Hs.553484	*ANGPT2*	Angiopoietin 2	5.34
Hs.209153	*ANGPTL3*	Angiopoietin-like 3	14.25
Hs.194654	*BAI1*	Brain-specific angiogenesis inhibitor 1	26.58
Hs.632586	*CXCL10*	Chemokine (C-X-C motif) ligand 10	18.47
Hs.89714	*CXCL5*	Chemokine (C-X-C motif) ligand 5	7.22
Hs.164021	*CXCL6*	Chemokine (C-X-C motif) ligand 6	15.22
Hs.77367	*CXCL9*	Chemokine (C-X-C motif) ligand 9	37.60
Hs.419815	*EGF*	Epidermal growth factor (β-urogastrone)	10.04
Hs.81071	*ECM1*	Extracellular matrix protein 1	4.28
Hs.483635	*FGF1*	Fibroblast growth factor 1 (acidic)	1.81
Hs.284244	*FGF2*	Fibroblast growth factor 2 (basic)	2.10
Hs.1420	*FGFR3*	Fibroblast growth factor receptor 3	18.22
Hs.160562	*IGF1*	Insulin-like growth factor 1 (somatomedin C)	12.53
Hs.1695	*MMP-12*	Matrix metallopeptidase 12 (macrophage elastase)	77.89
Hs.513617	*MMP-2*	Matrix metallopeptidase 2 (gelatinase A, 72-kDa type IV collagenase)	2.36
Hs.297413	*MMP-9*	Matrix metallopeptidase 9 (gelatinase B, 92-kDa type IV collagenase)	11.15
Hs.143436	*PLG*	Plasminogen	20.79
Hs.111779	*SPARC*	Secreted protein, acidic, cysteine-rich (osteonectin)	5.04
Hs.522632	*TIMP-1*	TIMP metallopeptidase inhibitor 1	6.08
Hs.633514	*TIMP-2*	TIMP metallopeptidase inhibitor 2	2.24
Genes down-regulated			
Hs.789	*CXCL1*	Chemokine (C-X-C motif) ligand 1 (melanoma growth stimulating activity, α)	2.74
Hs.89690	*CXCL3*	Chemokine (C-X-C motif) ligand 3	4.68
Hs.57697	*HAS1*	Hyaluronan synthase 1	19.58
Hs.482077	*ITGA2*	Integrin α_2 (CD49B, α2 subunit of VLA-2 receptor)	2.61
Hs.375957	*ITGB2*	Integrin β_2 (complement component 3 receptor 3 and 4 subunit)	31.16
Hs.126256	*IL1B*	Interleukin-1β	10.21
Hs.270364	*LAMA1*	Laminin α1	54.82
Hs.83169	*MMP-1*	Matrix metallopeptidase 1 (interstitial collagenase)	25.22

NOTE: U87 cells were treated with 5 mg/mL bevacizumab for 72 h. Treated cells represent cells that invaded across the transwell after treatment. mRNA and cDNA were obtained as described in Materials and Methods. Template cDNA (25 ng) was loaded in each real-time PCR reaction. Five housekeeping genes were used as controls for each gene expression calculation.

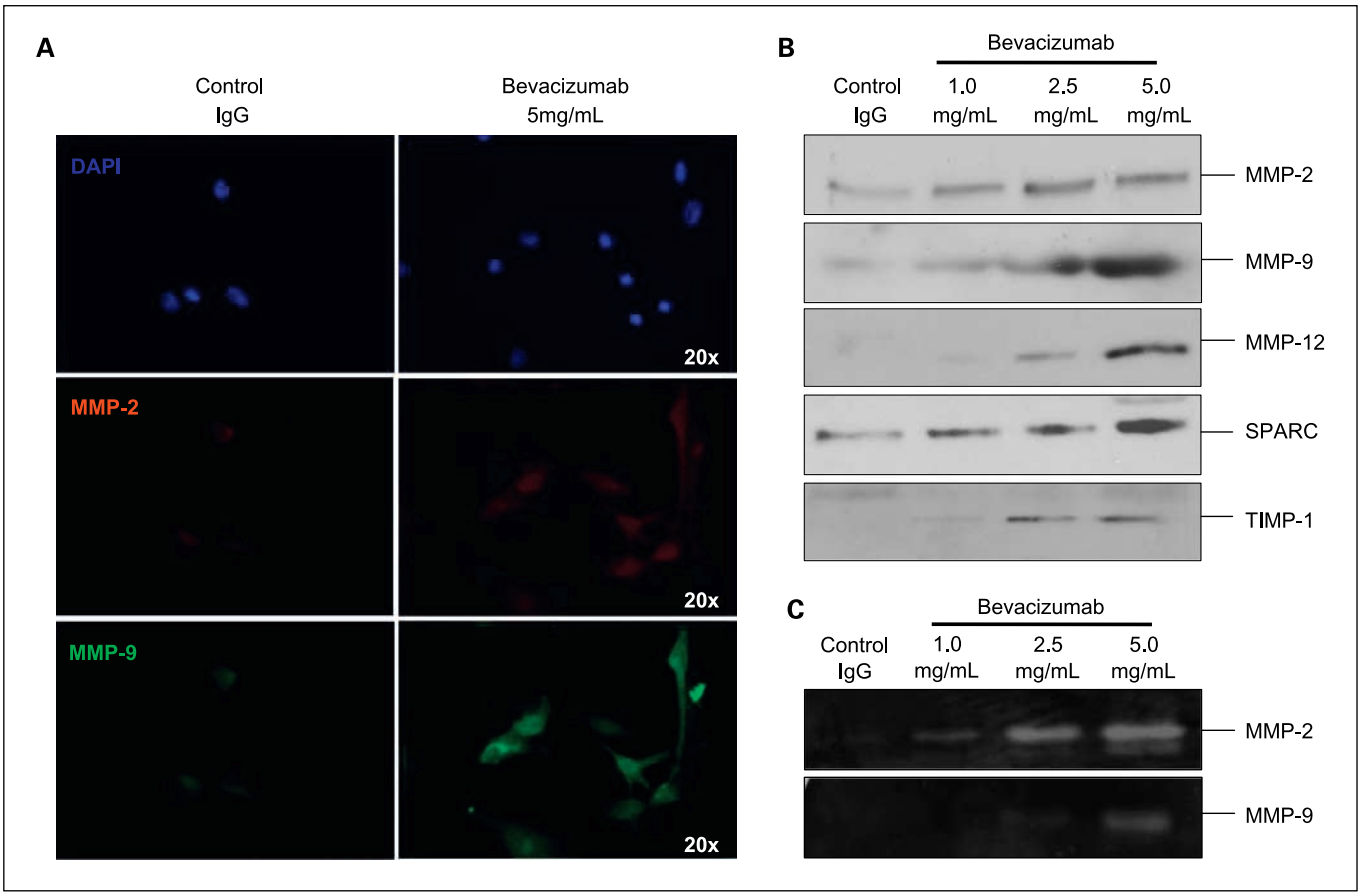

Fig. 2. Endogenous and secreted levels of invasion-related proteins are up-regulated after treatment with bevacizumab. *A,* immunofluorescence for MMP-2 and MMP-9 for control and bevacizumab-treated (5 mg/mL for 72 h) U87 cells. Primary antibody dilutions were 1:200 for MMP-2 and 1:300 for MMP-9. Pictures shown are the most representative from three independent experiments. *B,* Western blotting analyses of secreted proteins using conditioned media from U87 control and bevacizumab-treated cells. Primary antibody dilutions were, for MMP-2, 1:500; MMP-9, 1:400; MMP-12, 1:400; SPARC, 1:500; and TIMP-1, 1:400. *C,* gelatin zymography for MMP-2 and MMP-9 using conditioned media from control and bevacizumab-treated U87 cells. The loading amounts of proteins in *B* and *C* were normalized by the number of cells in each plate and also by protein quantification.

the endogenous and secreted protein levels, respectively, of MMP-2 and MMP-9. Figure 2A shows the immunofluorescence for MMP-2 and MMP-9 in U87 glioblastoma cell lines before and after bevacizumab treatment. We observed higher levels of endogenous MMP-2 and especially MMP-9 in the treated cells than in the control cells. The same result was obtained by Western blotting using conditioned media; thus, the secreted levels of MMP-2 and MMP-9 also were higher after bevacizumab treatment. In addition, secreted levels of invasion-related proteins MMP-12, SPARC, and TIMP-1 were also confirmed to be increased (Fig. 2B). These results validated the mRNA up-regulation shown by quantitative PCR.

As shown by Winkler et al. (9), besides its fundamental role in degrading ECM proteins, MMP-9 activity surrounding endothelial cells seems to be important for the normalization of abnormal tumor vasculature (through collagen degradation) during antiangiogenic treatment. To evaluate whether enzymatic activity of MMP-2 and MMP-9 was also increased with anti-VEGF treatment, we performed gelatin zymography using conditioned media from control and treated U87 and NSC23 cells. As expected, bevacizumab treatment increased the activity of both MMP-2 and MMP-9 (Fig. 2C).

***Anti-VEGF treatment promoted up-regulation of proangiogenic factors* in vitro.** To evaluate whether anti-VEGF treatment could lead to secretion of other proangiogenic factors as a compensatory mechanism of overcoming VEGF blockade, we analyzed the levels of multiple angiogenesis-related molecules secreted during anti-VEGF treatment in U87 and NSC23 cells. Figure 3 shows the results of angiogenesis antibody arrays using conditioned media. In U87 cells, after bevacizumab treatment, angiogenesis stimulators including angiogenin, interleukin-1α, and bFGF were up-regulated, whereas acidic FGF was down-regulated. Angiogenin and bFGF were also up-regulated in NSC23 cells after bevacizumab treatment, as were other proangiogenic molecules including acidic FGF, transforming growth factor α, and tumor necrosis factor α. Of all the proteins analyzed, angiogenin was the protein most up-regulated in U87 and NSC23 cells. Interestingly, for both cell lines, we also observed increased levels of the MMP inhibitors TIMP-1 (modest increase for U87 and significant increase for NSC23) and TIMP-2 (Fig. 3), which agreed with the data obtained by real-time PCR.

***VEGF blockade increased survival but leads to invasion* in vivo.** Because an increase in progression-free survival rates after antiangiogenic treatment has been shown in glioblastoma patients, we next examined the survival of nude mice with glioma xenografts after bevacizumab treatment. We observed

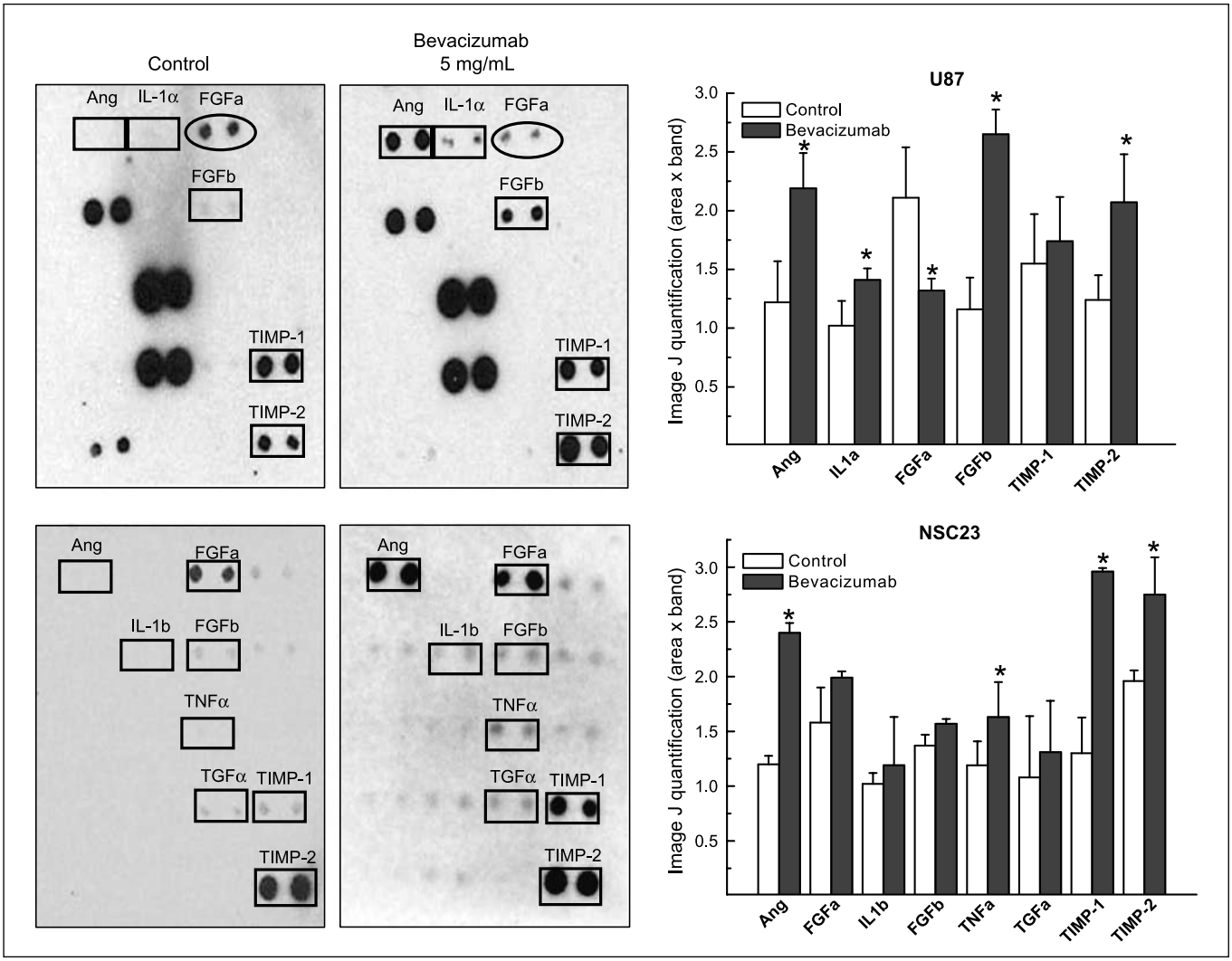

Fig. 3. Secreted proangiogenic factors are up-regulated following anti-VEGF treatment. Conditioned media (2 mL) from control and bevacizumab-treated (72 h) cells were incubated with Panomics angiogenesis antibody arrays for 2 h. Results are the most representative from three independent experiments. Highlighted proteins are angiogenin (*Ang*), interleukin-1α (*IL-1α*), interleukin-1β (*IL-1b*), acidic FGF (*FGFa*), bFGF (*FGFb*), tumor necrosis factor α (*TNFα*), transforming growth factor α (*TGFα*), TIMP-1, and TIMP-2. Square shapes, up-regulation; oval shapes, down-regulation. Graphs represent quantification of antibody array results using Image J software. *, $P < 0.05$, compared with control (Student's *t* test).

significant prolongation in animal survival after bevacizumab treatment (Fig. 4A). The median survival durations were 14 days for control mice treated with PBS/IgG and 47 days for mice treated with bevacizumab ($P < 0.004$). Not surprisingly, we observed a more invasive pattern of tumor growth after prolonged VEGF blockade than we did in control mice, echoing the results seen in our *in vitro* model. Whereas control tumors were circumscribed with well-defined edges, tumors in bevacizumab-treated animals displayed undefined edges and perivascular invasion, and satellite tumors were present far from the principal mass. Moreover, tumor cells and fingerlike extensions could be observed in the subpial surface of the brain in the treated xenografts (Fig. 4B, *bottom*). Another phenotypic alteration observed as a result of antiangiogenic treatment was a significantly higher number of necrotic regions than were seen in the control tumors, as shown in Fig. 4B (*top right, black arrow*).

To validate the increase in invasion-related proteins observed *in vitro*, we evaluated the levels of MMP-2, MMP-9, MMP-12, SPARC, and TIMP-1 in control and treated mice. Figure 4C shows the immunohistochemical results for these proteins in specimens obtained from our xenograft model. Notably, we observed higher levels of all of the invasion-related proteins in bevacizumab-treated animals than in control animals. These higher levels were detected not only in the principal tumor mass but also in the satellite and fingerlike invasive tumor cells.

Evasion of anti-VEGF treatment* in vivo *through alternate proangiogenic growth factors. bFGF has recently been shown to increase over time in patients with recurrent glioblastoma during treatment with the VEGFR inhibitor cediranib (24). To determine if evasion of bevacizumab therapy may also be mediated by bFGF, we analyzed by immunohistochemistry the levels of bFGF in specimens obtained from the U87 xenografts. Interestingly, although higher levels of bFGF were not observed after short-term VEGF blockade, at the time of tumor progression and animal death (7 weeks), a significant increase in this proangiogenic protein was observed (Fig. 5A). This result paralleled our *in vitro* findings and indicates the existence of a compensatory mechanism of enhancing angiogenesis, as

suggested by correlative observations in patients with glioblastoma (10).

To evaluate whether the tumor cells were, in fact, escaping from antiangiogenic treatment, we treated mice with bevacizumab for different times (4 and 7 weeks) and analyzed their tumor cell microvessel density compared with that in control animals. Immunostaining for factor VIII, a vessel density marker, showed that after 4 weeks of treatment, intratumoral microvessel density was significantly reduced (by 80%) in treated animals compared with that of the controls, an expected effect of antiangiogenic therapy. However, after 7 weeks of treatment, the pattern of microvessel density increased to levels higher than that observed in the control mice, clearly indicating that tumors could reactivate angiogenesis after long-term exposure to anti-VEGF therapy (Fig. 5B, *top*). The evasion of antiangiogenic treatment was also reflected by the levels of tumor cell proliferation. Although we observed a decrease (by 47%) in cell proliferation after short-term treatment, after 7 weeks, the proliferation increased to levels that were twice as high as that of the controls, as shown by Ki-67 staining (Fig. 5B, *bottom*).

***Anti-VEGF treatment induced hypoxia* in vivo.** The correlation between hypoxia and angiogenesis is well established; hypoxia can trigger angiogenesis by up-regulating VEGF expression (25–27). We evaluated the levels of hypoxia by immunohistochemical analysis using the hypoxia markers HIF-2α and CA IX in our xenograft model. Both proteins were up-regulated in short-term-treated tumors. At 7 weeks, there was a dramatic increase in levels of both HIF-2α and CA IX (Fig. 5C and D). We clearly observed these hypoxia-related proteins in and around necrotic tumor cells adjacent to areas of necrosis, suggesting that their up-regulation might be modulated, at least partially, by the deprivation of oxygenation and/or nutrients to the tumor. Interestingly, HIF-2α (Fig. 5C) and CA IX (Fig. 5D) staining in nonnecrotic regions and at earlier time points (at 4 weeks) was also observed, suggesting more widespread hypoxia in tissues without frank necrosis. Alternatively, an endogenous response to VEGF blockade could be to up-regulate these proteins.

MMP inhibitors prolonged the survival of bevacizumab-treated animals. To test whether the invasiveness caused by antiangiogenic treatment could be prevented, we tested combinations of

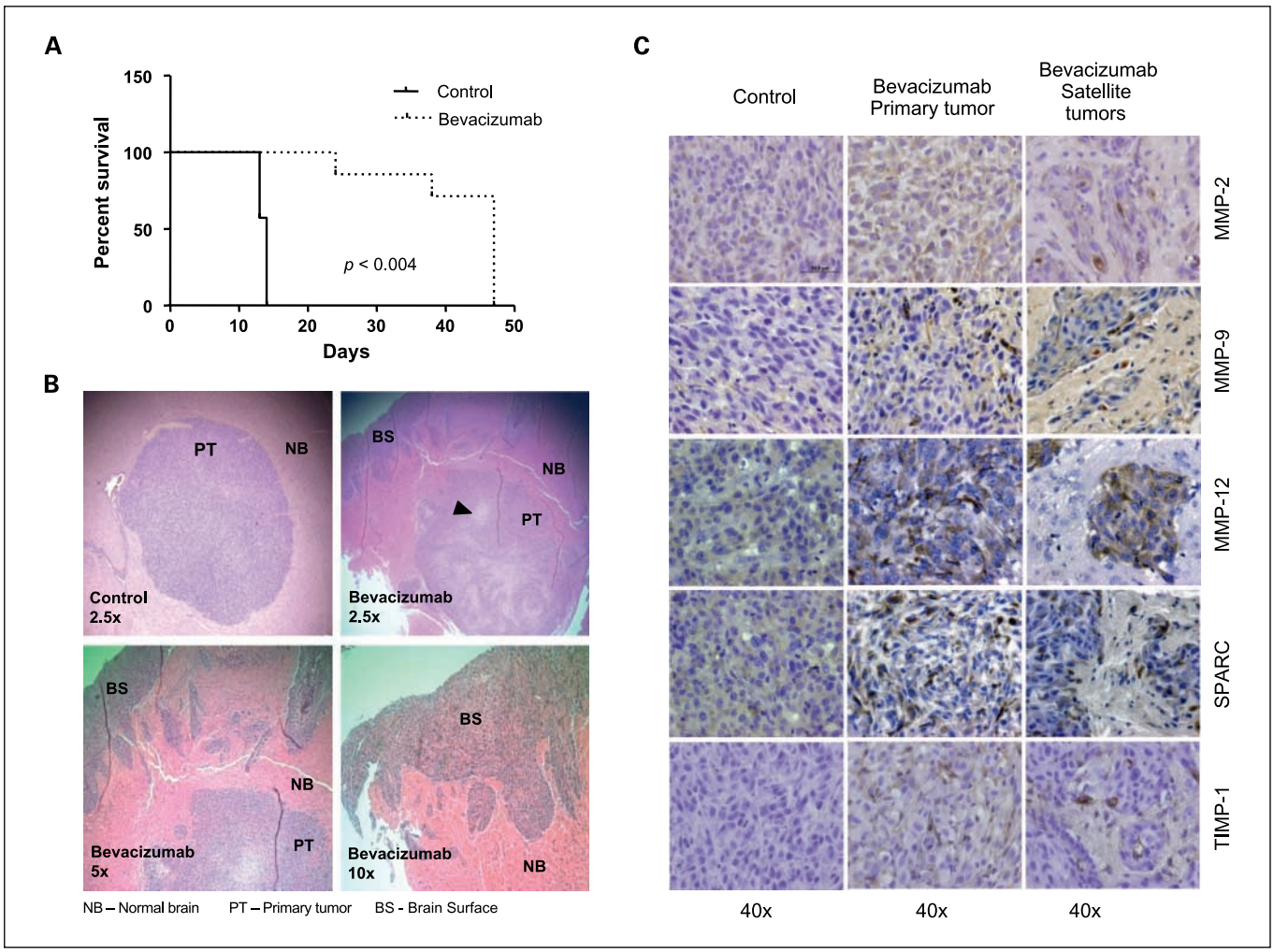

Fig. 4. VEGF blockade prolongs survival but increases invasion. *A,* Kaplan-Meier survival curves for control versus treated animals. *B,* top left, tumors in control animals with well-delineated margins; top right, tumors in bevacizumab-treated animals had numerous necrotic areas (*black arrow*) and were surrounded by multiple smaller satellite tumors. Bottom, higher magnification of bevacizumab-treated tumors showing the satellite tumors and tumor cells at the brain surface, some of them forming finger-like protrusions. *C,* immunohistochemical analysis of invasion-related proteins. Primary antibody dilutions were, for MMP-2, 1:50; MMP-9, 1:50; MMP-12, 1:200; SPARC, 1:100; and TIMP-1, 1:100.

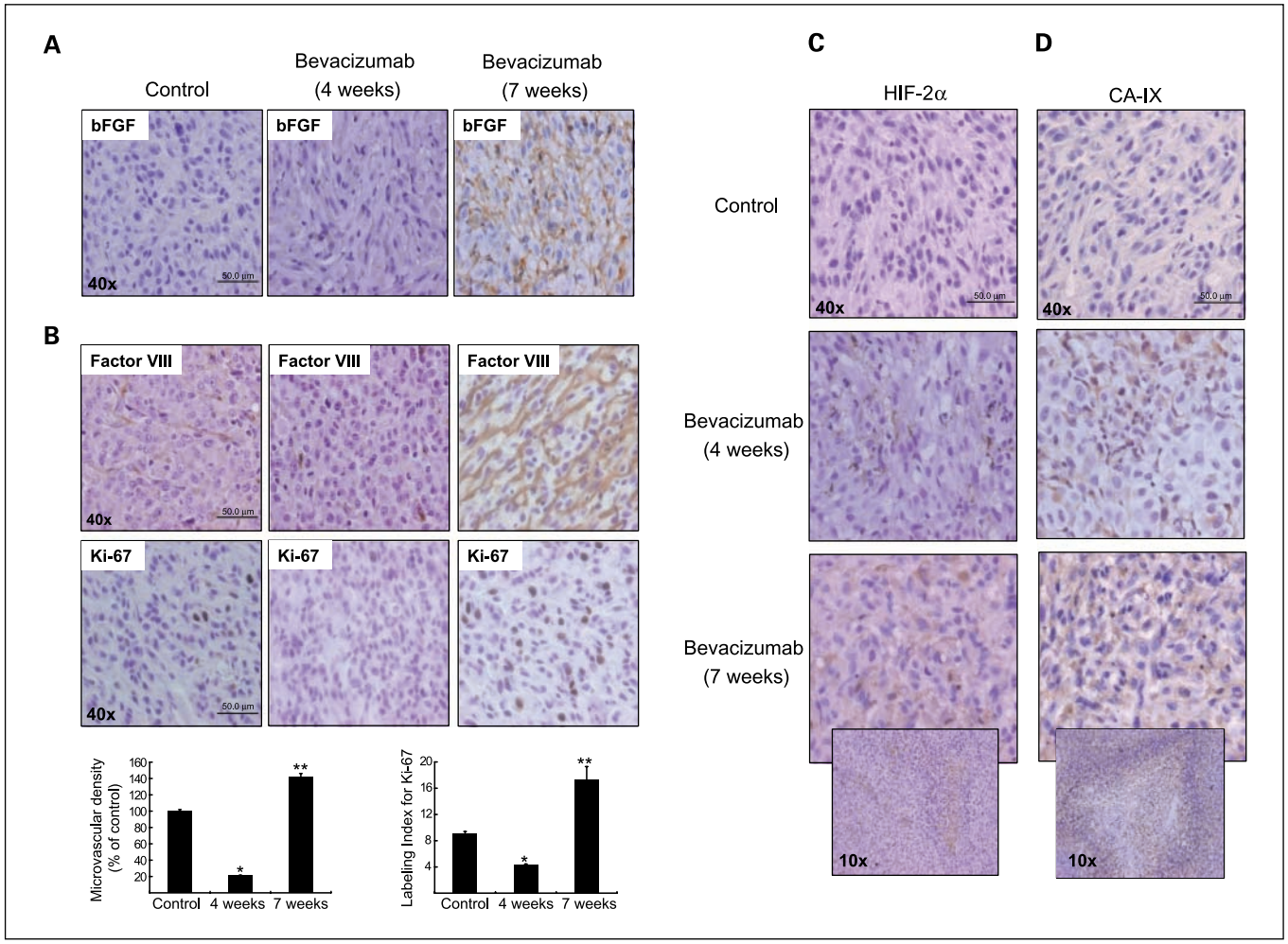

Fig. 5. Long-term VEGF blockade increases hypoxia and promotes escape from antiangiogenic treatment. *A,* immunostaining for bFGF in slides obtained from the glioblastoma xenografts. *B,* immunohistochemical detection of microvessel density (*factor VIII*) and proliferation (*Ki-67*) in glioblastoma xenografts. Microvascular density was quantified by counting the number of stained vessels per field (five fields were counted per sample at ×200 magnification) and are presented as percentage of control. Labeling index for Ki-67 was established as positively stained cancer cells that showed nuclear staining among 3,000 cancer cells counted in five fields at ×200 magnification. *, $P < 0.05$, compared with control; **, $P < 0.01$, compared with 4-wk treatment (Student's *t* test). *C* and *D,* immunohistochemical detection of hypoxic markers (HIF-2α and CA IX, respectively) in glioblastoma xenografts. Sections show stained cells adjacent to necrotic areas and also in perinecrotic regions after long-term bevacizumab treatment. Positive but less intense staining for HIF-2α and strong staining for CA IX were observed in both short-term and long-term bevacizumab-treated animals. Insets, pictures taken at ×100 magnification showing necrotic areas of the tumors.

two broad-spectrum MMP inhibitors (doxycycline and GM 6001) with bevacizumab both *in vitro* and *in vivo*. The Matrigel invasion assay in U87 cells showed a decrease in cellular invasion by 87% with the addition of doxycycline and by 68% with the addition of GM 6001, compared with invasion after bevacizumab alone (Fig. 6A). The cell viability for the control and bevacizumab-treated cells was very similar (not shown), indicating that the drug combinations had not had cytotoxic effects on the cells. In animals, the combination of bevacizumab with MMP inhibitors resulted in a longer median survival duration (39 days for doxycycline and 41.5 days for GM 6001) compared with that for bevacizumab alone [33.5 days; $P_{trend} < 0.05$, log-rank (Mantel Cox) test; Fig. 6B]. However, neither MMP inhibitor was effective in preventing tumor invasion *in vivo* (not shown), suggesting that the invasive process *in vivo* is highly complex and is difficult to block using inhibitors to one set of proteins. SPARC, TIMP-1, or other proteins (as shown previously) could play an important role in the invasiveness induced by anti-VEGF treatment *in vivo*.

Discussion

In the present study, we analyzed the effects of antiangiogenic therapy on tumor invasion, hypoxia, and evasion of anti-VEGF treatment in two glioblastoma cell lines. Using the anti-VEGF antibody bevacizumab, we first showed that bevacizumab was able to sequester the majority of secreted VEGF in U87 glioblastoma cells and in NSC23 glioma stem cells. This blockade increased invasion in glioblastoma cells in a concentration-dependent manner *in vitro*, suggesting that disruption of an autocrine loop may be important for the phenotypic change seen after antiangiogenic therapy. Moreover, we showed *in vitro* the up-regulation (mRNA and protein levels) of several important molecules related to angiogenesis (FGFs, interleukins, and angiogenin) and invasion (MMP-2, MMP-9, MMP-12, SPARC, and TIMPs). Collectively, these *in vitro* findings support the idea that glioblastoma cells can escape from antiangiogenic treatment

by up-regulating molecules that allow them to invade into surrounding brain areas.

Surprisingly, we showed a robust increase in invasion in the *in vitro* model due to the effects of anti-VEGF therapy as a result of the autocrine VEGF signaling blockade. Our data represent a clear indication that VEGF can influence glioblastoma cells directly and that the effects are not restricted to their influence on endothelial cells. The autocrine function of VEGF in cancer invasion was first shown in invasive breast carcinoma cell lines (3, 5). The authors of those studies proposed that this autocrine signaling contributes to tumor progression and motility by inducing chemokine receptor expression. While this article was in preparation, a study showing a correlation between the VEGF autocrine loop and malignant glioma viability and radioresistance was published (4), emphasizing the significance of this autocrine signaling loop in glioblastomas.

Using a glioblastoma xenograft model, we showed high levels of tumor invasion with multiple satellite tumors and finger-like tumor cells far from the principal mass after prolonged antiangiogenic treatment, although animal survival was up to 3.5 times longer in the treated group than in the control group. Higher levels of invasion-related proteins such as MMP-2, MMP-9, MMP-12, SPARC, and TIMPs were also observed in the treated tumors compared with levels in the controls, confirming the *in vitro* data.

Although the stimulus for this increased invasiveness *in vitro* and *in vivo* is still unknown, it is tempting to speculate that the decreased supply of oxygen and nutrients caused by prolonged antiangiogenic treatment may act as a stimulus for tumor cell migration. MMPs and other molecules could play an important role in promoting cell invasion into the surrounding brain. Our results show in different ways the overexpression of MMP-2 and MMP-9 both *in vitro* and *in vivo*, as well as their higher activity after bevacizumab treatment. MMPs may play other roles in glioblastoma resistance to antiangiogenic treatment. In addition to being implicated in degradation of ECM leading to cell invasion, MMPs can cleave protein substrates such as growth factors and their receptors, chemokines, and other MMPs, controlling cell proliferation. Moreover, MMPs can regulate angiogenesis by releasing VEGF and other growth factors from the ECM (28–34). MMP-9 has also been shown to be potentially important for reversing the abnormal vascular basement membrane thickness of glioblastoma vasculature, thus cooperating with anti-VEGF therapy in the process of vascular normalization (9). In that study, the activation of MMP-9 was achieved by the use of an antiangiogenic inhibitor (anti-VEGFR-2), a finding that is supported by our data.

In addition to showing that MMP-2 and MMP-9 were up-regulated in response to anti-VEGF therapy, we showed that other MMPs were increased. Although MMP-2 and MMP-9 are the most common metalloproteinases associated with neovascularization of tumors (29), our study showed that MMP-12 was highly up-regulated (mRNA levels of treated cells were 78 times higher than those of control cells), suggesting that this metalloproteinase could also play an important role in glioma invasion. MMP-12, also known as human macrophage

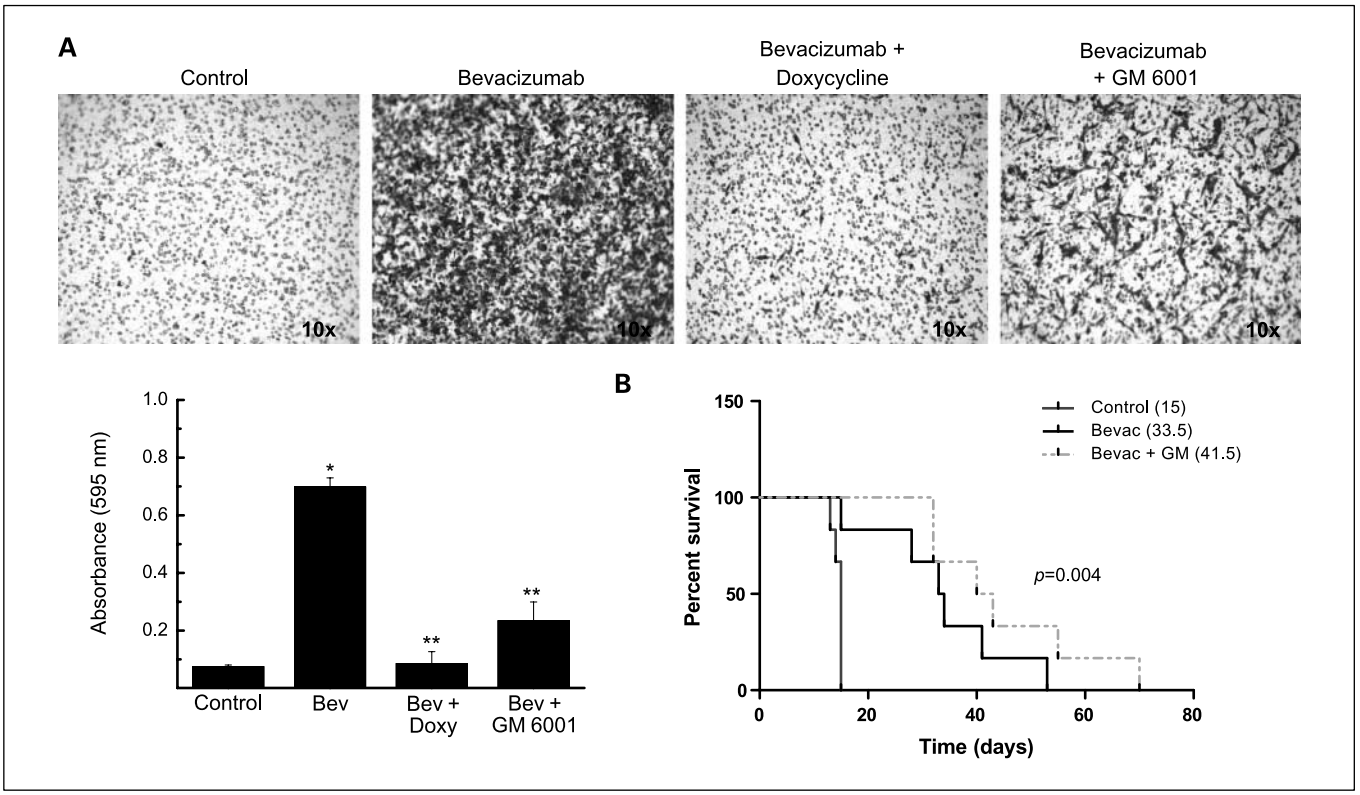

Fig. 6. MMP inhibitors prolong survival of bevacizumab-treated animals. *A,* Matrigel invasion assay for U87 glioblastoma cells treated with bevacizumab alone, bevacizumab plus doxycycline, and bevacizumab plus GM 6001. Cells (2.5×10^5) were allowed to invade for 24 h in serum-free medium. Pictures shown are the most representative from three independent experiments. The graph represents absorbance at 595 nm after incubation of the membranes with deoxycholic acid. *, $P < 0.01$, compared with control; **, $P < 0.01$, compared with bevacizumab alone (Student's *t* test). *B,* Kaplan-Meier survival curves for control versus treated mice. Numbers represent median survival (in days) for each animal group. The combination of bevacizumab with GM 6001 resulted in a longer median survival duration compared with control and bevacizumab alone [$P_{trend} = 0.004$, log-rank (Mantel Cox) test].

metalloelastase, is generally expressed by macrophages and is known to degrade multiple ECM substrates, including type IV collagen and myelin proteins such as myelin basic protein (35, 36). Anti-VEGF therapy is known to attract bone marrow–derived cells such as monocytes and macrophages to tumors (37), and it is interesting to speculate that MMP-12 release from tumor or tumor-associated macrophages might play an important role in this process. This is the first study showing a possible association between MMP-12 and antiangiogenesis treatment in glioblastoma.

Surprisingly, there was up-regulation of many other proangiogenic factors *in vitro*, and importantly, we show the up-regulation of bFGF *in vivo* after VEGF blockade. This observation confirms the suspicion that tumors are simultaneously developing mechanisms to escape from anti-VEGF agents via release of proangiogenic molecules as well as proinvasion mediators. We show the increase in blood vessel formation after long-term suppression of VEGF, although bevacizumab was able to decrease microvessel density in the short-term-treated tumors. The rapid increase in vascularity was shown to be associated with increased bFGF expression by immunohistochemistry. In the same way, a higher level of cellular proliferation after long-term antiangiogenic treatment was observed, another indication that the tumor cells had developed resistance to the treatment.

We propose that one mechanism by which tumor cells reactivate angiogenesis could be mediated by an increase in hypoxia, as shown by the up-regulation of hypoxia-associated markers HIF-2α and CA IX in this study. It has been suggested that pancreatic islet tumors escape from antiangiogenic treatment by this same mechanism (17). Hypoxia-triggered up-regulation of other proangiogenic factors may restimulate tumor angiogenesis. In accordance with their model, we showed that anti-VEGF therapy can increase hypoxia *in vivo*, which may be one trigger for the secretion of other proangiogenic factors (such as bFGF) that lead to evasion of anti-VEGF treatment.

It is important to emphasize that *in vitro*, our work showed that, besides bFGF, angiogenin seems to be the one of the most up-regulated secreted proteins after bevacizumab treatment, which might indicate an important function for this protein under autocrine VEGF blockade. Recent publications have shown that angiogenin can predict treatment response in stage IV melanoma patients (38) and also can be a prognostic factor for B-cell chronic lymphocytic leukemia (39). Other studies have shown the association between hypoxia and up-regulation of angiogenin in several types of cancer (40–43). The possible association between angiogenin and angiogenesis-triggered hypoxia and tumor escape from anti-VEGF therapy has never been shown in glioblastoma, revealing an interesting area for future investigation using angiogenin as a potential biomarker for glioblastoma escape from treatment.

Interestingly, we observed the up-regulation of both mRNA and protein levels of TIMPs during anti-VEGF therapy. These proteins have been described for many years as inhibitors of tumor growth, invasion, and metastasis through their role in inhibiting MMPs. However, recent publications have emphasized new important functions for TIMPs, describing them as multifunctional proteins (reviewed in refs. 44, 45). In addition, it has been postulated that increased TIMP-1 expression could be a response to (but not limited to) increased MMP levels in cancer cells (46). It should also be noted that increased TIMP-1 levels are associated with a poor prognosis in multiple cancer types (47). The up-regulation of TIMPs in the setting of anti-VEGF therapy may show an association with an increase in MMP secretion and could be a marker of the phenotypic change in tumor behavior toward a more aggressive and invasive tumor.

Finally, we showed that the concomitant use of broad-spectrum MMP inhibitors with bevacizumab significantly increased the median survival of animals with tumors and decreased glioblastoma invasion *in vitro*. However, this combination therapy did not prevent increased invasion *in vivo*. Obviously, tumor invasion *in vivo* involves multiple complicated and overlapping mechanisms, including cell detachment, anchorage to ECM, remodeling of the ECM, the multiple steps in cell migration (reviewed in ref. 48). Therefore, the use of MMP inhibitors as a purely anti-invasive therapy might not be enough to prevent anti-VEGF–driven invasion. Importantly, MMPs have a clearly defined role in promoting angiogenesis by releasing proangiogenic factors from ECM. Thus, our results indicate that the combination of anti-VEGF therapy with inhibitors of MMP is a reasonable approach to the treatment of glioblastoma and may represent dual inhibition of angiogenesis rather than a combination that blocks tumor invasion. The use of doxycycline as an antiangiogenesis treatment was corroborated by the recent report by Fainaru et al. (49), who showed that doxycycline prevents vascular hyperpermeability in tumors and can decrease tumor volume *in vivo*.

In conclusion, this work shows the importance of both autocrine and paracrine VEGF signaling in mediating tumor evasion of anti-VEGF therapy. Our identification of potential mediators of the mechanisms of escape from anti-VEGF therapy is a first step in developing novel combination therapies to overcome the resistance phenotype. The long-term success of antiangiogenic agents in the clinic will depend on our ability to control tumor migration. Clinical trials designed to block both VEGF and tumor invasion are currently under development for recurrent glioblastoma.

Disclosure of Potential Conflicts of Interest

J. de Groot, commercial research grant, Adnexus; advisory board, Exelixis.

References

1. Ferrara N. Vascular endothelial growth factor: basic science and clinical progress. Endocr Rev 2004;25:581–611.
2. Hicklin DJ, Ellis LM. Role of the vascular endothelial growth factor pathway in tumor growth and angiogenesis. J Clin Oncol 2005;23:1011–27.
3. Bachelder RE, Wendt MA, Mercurio AM. Vascular endothelial growth factor promotes breast carcinoma invasion in an autocrine manner by regulating the chemokine receptor CXCR4. Cancer Res 2002;62:7203–6.
4. Knizetova P, Ehrmann J, Hlobilkova A, et al. Autocrine regulation of glioblastoma cell cycle progression, viability and radioresistance through the VEGF-VEGFR2 (KDR) interplay. Cell Cycle 2008;7:2553–61.
5. Price DJ, Miralem T, Jiang S, Steinberg R, Avraham H. Role of vascular endothelial growth factor in the stimulation of cellular invasion and signaling of breast cancer cells. Cell Growth Differ 2001;12:129–35.
6. Grunwald V, Hidalgo M. Developing inhibitors of the epidermal growth factor receptor for cancer treatment. J Natl Cancer Inst 2003;95:851–67.
7. Prewett M, Huber J, Li Y, et al. Antivascular endothelial growth factor receptor (fetal liver kinase 1) monoclonal

antibody inhibits tumor angiogenesis and growth of several mouse and human tumors. Cancer Res 1999; 59:5209–18.

8. Viloria-Petit A, Crombet T, Jothy S, et al. Acquired resistance to the antitumor effect of epidermal growth factor receptor-blocking antibodies *in vivo*: a role for altered tumor angiogenesis. Cancer Res 2001;61: 5090–101.

9. Winkler F, Kozin SV, Tong RT, et al. Kinetics of vascular normalization by VEGFR2 blockade governs brain tumor response to radiation: role of oxygenation, angiopoietin-1, and matrix metalloproteinases. Cancer Cell 2004;6:553–63.

10. Gerstner ER, Duda DG, di Tomaso E, et al. Antiangiogenic agents for the treatment of glioblastoma. Expert Opin Investig Drugs 2007;16:1895–908.

11. Jain RK. Normalizing tumor vasculature with anti-angiogenic therapy: a new paradigm for combination therapy. Nat Med 2001;7:987–9.

12. Jain RK, Duda DG, Clark JW, Loeffler JS. Lessons from phase III clinical trials on anti-VEGF therapy for cancer. Nat Clin Pract Oncol 2006;3:24–40.

13. Vredenburgh JJ, Desjardins A, Herndon JE II, et al. Bevacizumab plus irinotecan in recurrent glioblastoma multiforme. J Clin Oncol 2007;25:4722–9.

14. Cloughesy TF, Prados MD, Wen PY, et al. A phase II, andomized, non-comparative clinical trial of the effect of bevacizumab (BV) alone or in combination with irinotecan (CPT) on 6-month progression free survival (PFS6) in recurrent, treatment-refractory glioblastoma (GBM) [abstract 2010b]. J Clin Oncol 2008;26.

15. Miller KD, Chap LI, Holmes FA, et al. Randomized phase III trial of capecitabine compared with bevacizumab plus capecitabine in patients with previously treated metastatic breast cancer. J Clin Oncol 2005; 23:792–9.

16. Hurwitz H, Fehrenbacher L, Novotny W, et al. Bevacizumab plus irinotecan, fluorouracil, and leucovorin for metastatic colorectal cancer. N Engl J Med 2004; 350:2335–42.

17. Casanovas O, Hicklin DJ, Bergers G, Hanahan D. Drug resistance by evasion of antiangiogenic targeting of VEGF signaling in late-stage pancreatic islet tumors. Cancer Cell 2005;8:299–309.

18. Kunkel P, Ulbricht U, Bohlen P, et al. Inhibition of glioma angiogenesis and growth *in vivo* by systemic treatment with a monoclonal antibody against vascular endothelial growth factor receptor-2. Cancer Res 2001;61:6624–8.

19. Lamszus K, Kunkel P, Westphal M. Invasion as limitation to anti-angiogenic glioma therapy. Acta Neurochir Suppl 2003;88:169–77.

20. Norden AD, Young GS, Setayesh K, et al. Bevacizumab for recurrent malignant gliomas: efficacy, toxicity, and patterns of recurrence. Neurology 2008;70: 779–87.

21. Loupakis F, Falcone A, Masi G, et al. Vascular endothelial growth factor levels in immunodepleted plasma of cancer patients as a possible pharmacodynamic marker for bevacizumab activity. J Clin Oncol 2007; 25:1816–8.

22. Laemmli UK. Cleavage of structural proteins during the assembly of the head of bacteriophage T4. Nature 1970;227:680–5.

23. Georgescu MM, Kirsch KH, Kaloudis P, et al. Stabilization and productive positioning roles of the C2 domain of PTEN tumor suppressor. Cancer Res 2000; 60:7033–8.

24. Batchelor TT, Sorensen AG, di Tomaso E, et al. AZD2171, a pan-VEGF receptor tyrosine kinase inhibitor, normalizes tumor vasculature and alleviates edema in glioblastoma patients. Cancer Cell 2007;11:83–95.

25. Carmeliet P, Dor Y, Herbert JM, et al. Role of HIF-1α in hypoxia-mediated apoptosis, cell proliferation and tumour angiogenesis. Nature 1998;394:485–90.

26. Forsythe JA, Jiang BH, Iyer NV, et al. Activation of vascular endothelial growth factor gene transcription by hypoxia-inducible factor 1. Mol Cell Biol 1996;16: 4604–13.

27. Maxwell PH, Dachs GU, Gleadle JM, et al. Hypoxia-inducible factor-1 modulates gene expression in solid tumors and influences both angiogenesis and tumor growth. Proc Natl Acad Sci U S A 1997;94: 8104–9.

28. Chambers AF, Matrisian LM. Changing views of the role of matrix metalloproteinases in metastasis. J Natl Cancer Inst 1997;89:1260–70.

29. Djonov V, Cresto N, Aebersold DM, et al. Tumor cell specific expression of MMP-2 correlates with tumor vascularisation in breast cancer. Int J Oncol 2002;21: 25–30.

30. Du R, Petritsch C, Lu K, et al. Matrix metalloproteinase-2 regulates vascular patterning and growth affecting tumor cell survival and invasion in GBM. Neuro-oncol 2008;10:254–64.

31. Duffy MJ, McGowan PM, Gallagher WM. Cancer invasion and metastasis: changing views. J Pathol 2008;214:283–93.

32. Egeblad M, Werb Z. New functions for the matrix metalloproteinases in cancer progression. Nat Rev Cancer 2002;2:161–74.

33. Mott JD, Werb Z. Regulation of matrix biology by matrix metalloproteinases. Curr Opin Cell Biol 2004; 16:558–64.

34. Page-McCaw A, Ewald AJ, Werb Z. Matrix metalloproteinases and the regulation of tissue remodelling. Nat Rev Mol Cell Biol 2007;8:221–33.

35. Chandler S, Cossins J, Lury J, Wells G. Macrophage metalloelastase degrades matrix and myelin proteins and processes a tumour necrosis factor-α fusion protein. Biochem Biophys Res Commun 1996;228:421–9.

36. Shapiro SD, Kobayashi DK, Pentland AP, Welgus HG. Induction of macrophage metalloproteinases by extracellular matrix. Evidence for enzyme- and substrate-specific responses involving prostaglandin-dependent mechanisms. J Biol Chem 1993;268: 8170–5.

37. Bergers G, Hanahan D. Modes of resistance to anti-angiogenic therapy. Nat Rev Cancer 2008;8: 592–603.

38. Vihinen P, Kallioinen M, Vuoristo MS, et al. Serum angiogenin levels predict treatment response in patients with stage IV melanoma. Clin Exp Metastasis 2007;24:567–74.

39. Molica S, Vitelli G, Levato D, et al. Serum angiogenin is not elevated in patients with early B-cell chronic lymphocytic leukemia but is prognostic factor for disease progression. Eur J Haematol 2004;73:36–42.

40. Campo L, Turley H, Han C, et al. Angiogenin is up-regulated in the nucleus and cytoplasm in human primary breast carcinoma and is associated with markers of hypoxia but not survival. J Pathol 2005; 205:585–91.

41. Hartmann A, Kunz M, Kostlin S, et al. Hypoxia-induced up-regulation of angiogenin in human malignant melanoma. Cancer Res 1999;59:1578–83.

42. Nakamura M, Yamabe H, Osawa H, et al. Hypoxic conditions stimulate the production of angiogenin and vascular endothelial growth factor by human renal proximal tubular epithelial cells in culture. Nephrol Dial Transplant 2006;21:1489–95.

43. Pilch H, Schlenger K, Steiner E, et al. Hypoxia-stimulated expression of angiogenic growth factors in cervical cancer cells and cervical cancer-derived fibroblasts. Int J Gynecol Cancer 2001;11:137–42.

44. Chirco R, Liu XW, Jung KK, Kim HR. Novel functions of TIMPs in cell signaling. Cancer Metastasis Rev 2006;25:99–113.

45. Jiang Y, Goldberg ID, Shi YE. Complex roles of tissue inhibitors of metalloproteinases in cancer. Oncogene 2002;21:2245–52.

46. Bachmeier BE, Vene R, Iancu CM, et al. Transcriptional control of cell density dependent regulation of matrix metalloproteinase and TIMP expression in breast cancer cell lines. Thromb Haemost 2005;93: 761–9.

47. Hornebeck W, Lambert E, Petitfrere E, Bernard P. Beneficial and detrimental influences of tissue inhibitor of metalloproteinase-1 (TIMP-1) in tumor progression. Biochimie 2005;87:377–83.

48. Nakada M, Nakada S, Demuth T, et al. Molecular targets of glioma invasion. Cell Mol Life Sci 2007;64: 458–78.

49. Fainaru O, Adini I, Benny O, et al. Doxycycline induces membrane expression of VE-cadherin on endothelial cells and prevents vascular hyperpermeability. FASEB J 2008;22:3728–35.

Clinical Cancer Research

Mediators of Glioblastoma Resistance and Invasion during Antivascular Endothelial Growth Factor Therapy

Agda K. Lucio-Eterovic, Yuji Piao and John F. de Groot

Clin Cancer Res 2009;15:4589-4599.